Joint estimation of image rotation angle and scaling factor

Kun Yu, Rongsong Yang, Hui Zeng and Anjie Peng
School of Computer Science & Technology Southwest University of Science and Technology Mianyang, China
zengh5@mail2.sysu.edu.cn

***Abstract*— Scaling and rotation are often involved in image tampering, and thus have attracted wide attention in image forensics. However, existing studies usually focus on detection or parameter estimation of a single operation, e. g., scaling or rotation. When a probe image has been both scaled and rotated, the statistical characteristics on which previous methods are based become much complicated and the parameter estimation task becomes much challenging. By analyzing the interaction between the features of both operations, a joint parameter estimation method is proposed in this paper. Firstly, some candidate estimations of the rotation angle are derived from the cyclic spectrum of the questioned image. Then, by taking the dependence between the peaks caused by rotation and those caused by scaling-then-rotation into consideration, these candidates can be further checked. Finally, both the scaling factor and the rotation angle can be derived with the proposed method. The proposed method is verified by conducting experiments on a subset of the BOSSbase dataset, achieves accuracy of 84.96% in rotation angle estimation, 78.88% in scaling factor estimation, and 77.13% in the estimation of both parameters.**

***Index Terms*—Image tampering, scaling factor estimation, rotation angle estimation, cyclic spectrum, joint parameter estimation**

I. INTRODUCTION

Image tampering is usually accompanied by the whole or local geometric transformation, such as scaling and rotation. Revealing a localized geometric transformation and possibly further estimating its exact parameters can provide meaningful clues for forensic analysis [1-4]. Previous studies revealed that both scaling and rotation introduce periodic artifacts into resampled images, which is an important fingerprint for resampling detection [1, 2]. Such periodic artifacts can be manifested by p-map [2], variance [1, 3], edge map [13], or cyclic correlation [5]. By searching the location of the peaks in the spectrum, the exact scaling factor or rotation angle can be estimated.

However, most of the previous works only studied the characteristics introduced by a single operation, scaling or rotation. Due to the fact that the forensic features introduced by scaling and rotation are likely to interfere with each other, these methods cannot directly extend to images that have been both scaled and rotated, which motivated this work.

During studying of a scaled then rotated image, we find that the forensic features introduced by these successive operations are strongly correlated. By taking such correlation into geometric transform parameter estimation, the false features can be avoided significantly, and the estimation accuracy can be improved. Experiments on a public database verified the effectiveness and the advantage to the state of the arts of the proposed method.

The rest of this paper is organized as follows. In the Section II, we review the existing works on image scaling factor estimation and rotation angle estimation. In the Section III, we analyze the interference between both operations in the feature domain and propose a joint estimation method for scaling factor and rotation angle. Experiments are presented in the fourth Section IV. The paper is closed in the Section V.

II. BACKGROUND AND RELATED WORK

A. Periodicity artifacts due to resampling

Generally speaking, resampling and interpolation are involved during image geometric transform. Let the coordinate of a pixel in the original image be $\boldsymbol{x} = (x_1, x_2)$, and the corresponding coordinates of this pixel in the resampled image be $\boldsymbol{y} = (y_1, y_2)$, the resampling operation can be expressed as

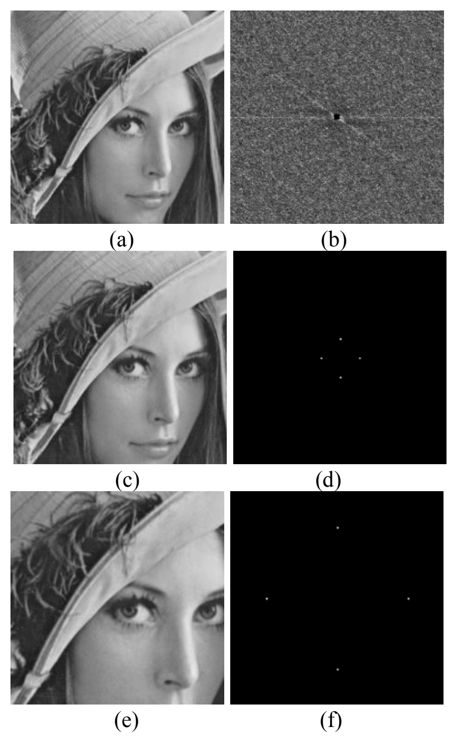

Fig. 1 Scaling factor estimation based on periodicity artifacts. (a) Original image, (b) the spectrum calculated on (a) using the method in [6], (c) upsampling image with a factor of 1.1, (d) the spectrum calculated on (c), (e) upsampling image with a factor of 1.5, (f) the spectrum calculated on (e).

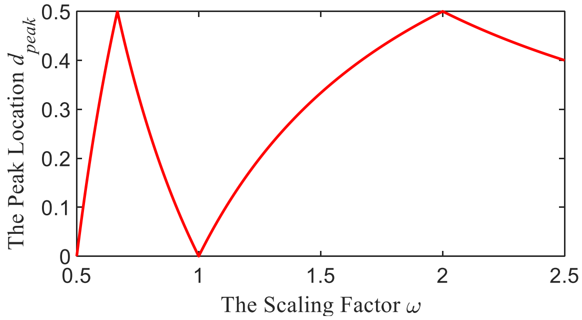

Fig. 2 The peak location d_{peak} as a function of the scaling factor $\omega \in (0.5,\ 2.5)$.

$$\boldsymbol{y} = \boldsymbol{Hx}, \tag{1}$$

where $\boldsymbol{H}$ is the affine transformation matrix. Without loss of generality, we assume isotropic scaling and ignore the translation, the transformation matrix can be written as

$$\boldsymbol{H} = \begin{bmatrix} \omega \cdot \cos\theta & \omega \cdot -\sin\theta \\ \omega \cdot \sin\theta & \omega \cdot \cos\theta \end{bmatrix}, \tag{2}$$

where ω is the scaling factor and θ is the rotation angle. Since the mapping above is from integer value to real value, i. e., $\mathbb{Z}^2 \to \mathbb{R}^2$, most pixels in the target image cannot find their exact counterparts. Thus interpolation is needed for calculating the values of these pixels. Previous studies [1, 2] found that such interpolation process will introduce periodicity artifacts that can be used for resampling detection. In [2, 6], this periodicity artifacts is manifested by the Fourier transform of the residue of a local linear predictor. As shown in Fig. 1(d) and (f), there are obvious bright peaks in the spectrum of the resampled images, which imply the periodicity of the spatial domain.

B. *Resampling parameter estimation*

Staring from spectrum representation of the periodicity artifacts, several works are dedicated to estimate the exact geometric parameters, i.e., scaling factor and rotation angle.

For upscaled images, i.e., $\omega > 1$, Gallagher found that the relationship between scaling factor and expected position of resampling peaks d_{peak} can be expressed as follows [1]:

$$d_{peak} = \begin{cases} \dfrac{\omega - 1}{\omega}, & 1 < \omega < 2 \\ \dfrac{1}{\omega}, & \omega \geq 2 \end{cases}, \tag{3}$$

In [7], such relationship is extended to arbitrary ω as:

$$d_{peak} = \left|\frac{1}{\omega}\right| - round\left(\frac{1}{\omega}\right) \tag{4}$$

In Fig. 2, the relationship (4) is plotted for $\omega > 0.5$. It is observed that a detected peak location can be introduced by several candidate scaling factors. For example, in the case of $\omega = 3/4$, $\omega = 3/2$, and $\omega = 3$, all the expected d_{peak}s equal to $1/3$. To address this ambiguity, an energy-based method [8] can be used to determine the interval of the scaling factor. To simplify the further analysis, in this paper, we restrict the scaling factor into $[1, 2)$, in which we have $\omega = 1/(1 - d_{peak})$ according to (3). However, the method proposed in the next section can be extended to other intervals by combining the method in [8].

In [5], the cyclic spectrum is used to detect the periodicity caused by resampling instead of the p-map in the Fourier domain. Experimental results showed its superiority in estimating the parameters of spatially transformed images. In [9], the accuracy of rotation angle estimation is improved by only searching peaks along four trajectories instead of the entire spectrum. The authors of [9] also pointed out that normalizing the frequency to $[0, 1)^2$ rather than $[-0.5, 0.5)^2$ is helpful to analyze the rotation angle. Fig. 3 shows the peak trajectories in cyclic spectrum caused by

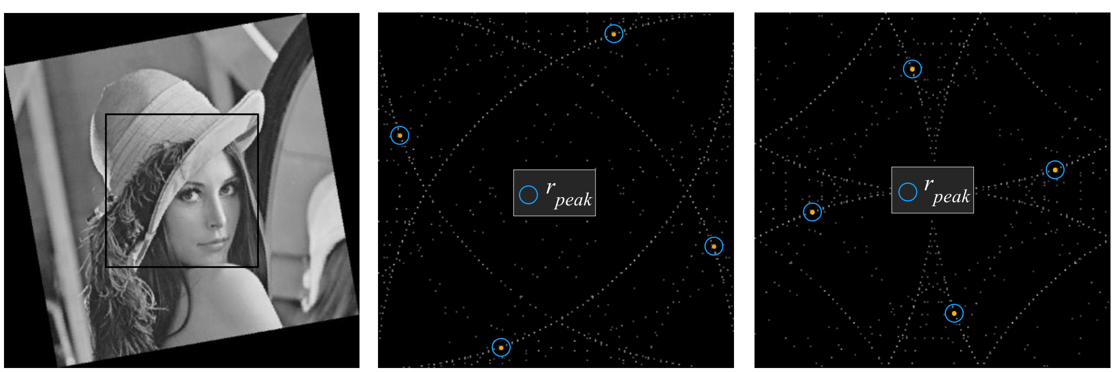

(a) (b) (c)

Fig. 3 Rotating angle estimation based on the peak trajectories. (a) Lena image rotated by $\theta = 20°$, the analysis block of the size 256×256 is inside the frame, (b) and (c) are the frequency domain images of the statistics of (a), the normalized frequencies are respectively $[0, 1)^2$(b) and $[-0.5, 0.5)^2$(c). The white dashed lines illustrate the peak trajectories when θ varies from 0° to 90° with a step of 1°.

rotation. As shown in Fig. 3(b), when the frequency is normalized to $[0,1)^2$, the peak trajectories are four quarter arcs centered in the four corners.

$$\begin{aligned} \boldsymbol{l}_\theta^{(1,0)}&: f_x^2+f_y^2=1, \\ \boldsymbol{l}_\theta^{(-1,0)}&: (1-f_x)^2+(1-f_y)^2=1, \\ \boldsymbol{l}_\theta^{(0,1)}&: (1-f_x)^2+f_y^2=1, \\ \boldsymbol{l}_\theta^{(0,-1)}&: f_x^2+(1-f_y)^2=1. \end{aligned} \tag{5}$$

where $0 \leqslant f_x \leqslant 1, 0 \leqslant f_y \leqslant 1$ are the normalized frequencies. The rotation angle can be estimated as $\hat{\theta}=-arctan(f_y/f_x)$. If the frequency is normalized to $[-0.5,0.5)^2$ as that in Fig. 3(c), the analysis will be more complicated. Hence, in the next Section, we will follow [9] to normalize the spectrum to $[0,1)^2$. In [10], Dai preprocessed the cyclic spectrum with wavelet denoising to eliminate the block artefacts brought by JPEG compression.

All the works reviewed above are only for image after single geometric transform, e.g., resizing or rotation. To our best knowledge, the only existing work that can estimate the exact parameters from an image undergone successive geometric transform is [12]. In [12], 12 theoretical peak positions of each combination of (ω,θ) are calculated to build a reference table. For a probe image, its spectrum is binarized with a threshold τ, and matched with the reference table. The combination of (ω,θ) that results most matches is regarded as the parameter estimation result.

III. PROPOSED METHOD

In practice, scaling and rotation are often used together during image tampering. In this case, the periodicity artifacts caused by the first operation will be weakened by the latter operation. Moreover, the artifacts caused by both operations will interfere with each other. Our preliminary experiments suggest that the case of an image is first rotated and then scaled is rather complicated. Thus we would like to leave it for future study. In this study, we focus on the case that an image is scaled then rotated. As shown in Fig. 4, except for the peaks corresponding to rotation (blue circles), there are also peaks caused by scaling-then-rotation (yellow circles). The first type of peaks is expressed in [9], and the functions of the latter type of peaks can be expressed as follows:

$$\begin{aligned} \boldsymbol{s}_{peak}^{(1,0)}&=l_r(\cos\theta,-\sin\theta), \\ \boldsymbol{s}_{peak}^{(-1,0)}&=l_r(1-\cos\theta,1+\sin\theta), \\ \boldsymbol{s}_{peak}^{(0,1)}&=l_r(1+\sin\theta,\cos\theta), \\ \boldsymbol{s}_{peak}^{(0,-1)}&=l_r(-\sin\theta,1-\cos\theta), \end{aligned} \tag{6}$$

where $l_r=(\omega-1)/\omega$. When θ varies from 0° to 90°, these resampling peaks leave four trajectory curves in the spectrum.

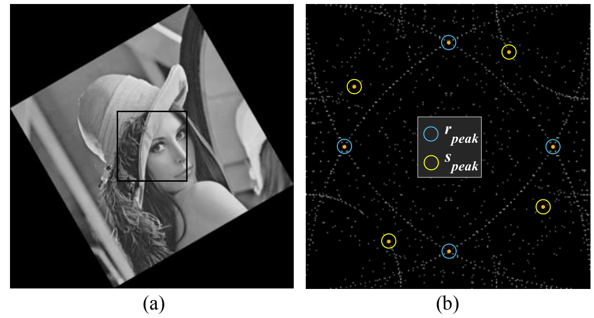

Fig. 4 Spectrum analysis of an image after scaling-then-rotation. (a) a probe image, which is created from the Lena image by scaling with a factor of 1.5 and rotating by 30 degrees, only the center block with the size of 256 by 256 pixels is analyzed. (b) the spectrum obtained with the method in [5]. The frequency is normalized to $[0,1)^2$.

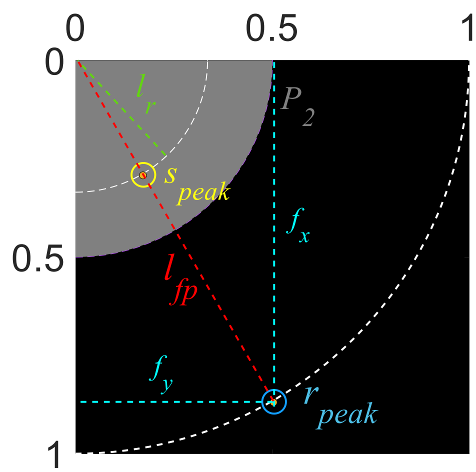

Fig. 5 Illustration of the proposed joint estimation scheme for scaling factor and rotation angle. Candidate $\boldsymbol{r}_{peak}$ s are first searched along the outer arc, and further checked by whether a $\boldsymbol{s}_{peak}$ located in the line determined by (0, 0) and $\boldsymbol{r}_{peak}$.

$$\begin{aligned} \boldsymbol{l}_\omega^{(1,0)}&: f_x^2+f_y^2=l_r, \\ \boldsymbol{l}_\omega^{(-1,0)}&: (1-f_x)^2+(1-f_y)^2=l_r, \\ \boldsymbol{l}_\omega^{(0,1)}&: (1-f_x)^2+f_y^2=l_r, \\ \boldsymbol{l}_\omega^{(0,-1)}&: f_x^2+(1-f_y)^2=l_r. \end{aligned} \tag{7}$$

Moreover, by comparing (5) and (6), we can observe that the peaks of the latter type locate on the lines determined by the peaks of the first type and four corners. For example, $\boldsymbol{s}_{peak}^{(1,0)}$ locates on the line determined by $(0,0)$ and $(cos\theta,-sin\theta)$. This can be explained as follows. The first scaling introduces peaks which located on the borders of the spectrum. Since rotation in spatial domain equals to rotation in frequency domain, these peaks will be rotated to the inside of the spectrum from the borders, with the same angle of the spatial domain. Such location dependencies is critical to the algorithm

---

Algorithm 1

Input: the cyclic spectrum Txx of a probe image $\boldsymbol{I}$;

1. Normalize Txx to $[0, 1)^2$.

2. Find $\boldsymbol{r}_{peak}(n), n \in [0 \ldots N]$ along $\boldsymbol{l}_\theta$ in Txx, which satisfy $\boldsymbol{r}_{peak}(n) > t_1$.

3. If $n = 0$, then $\hat{\theta} = 0°$, $\hat{\omega} = 1$, END. Otherwise, sort $\boldsymbol{r}_{peak}(n)$ in descending order, go to step 4.

4. For $m = 1$ to n

$\boldsymbol{r}_{temp} = \boldsymbol{r}_{peak}(m)$;

if existing $\boldsymbol{s}_{peak} > t_2$ in $\boldsymbol{P}_2$ and $\boldsymbol{s}_{peak}$ located on the line $\boldsymbol{l}_{fp}$ determined by $(0,0)$ and $\boldsymbol{r}_{temp}$, then calculate $\hat{\theta}$ according to $\boldsymbol{r}_{temp}$, go to step 6.

5. $\boldsymbol{r}_{temp} = max(\boldsymbol{r}_{peak}(n))$, calculate $\hat{\theta}$ according to $\boldsymbol{r}_{temp}$, $\hat{\omega} = 1$, END.

6. Get the distance $\boldsymbol{l}_r$ between $(0,0)$ and $\boldsymbol{s}_{peak}$, calculate the candidate $\hat{\omega} = 1/(1 - l_r)$.

$\boldsymbol{l}_\theta$ are the four trajectories described in (5).

N is the number of candidate peaks.

t_1, t_2 are the thresholds of peak detector.

$\boldsymbol{P}_2$ is a 90-degree sector illustrated as gray area in Fig. 5. Note $x = 0$ and $y = 0$ are excluded.

---

that we are going to come up with. Fig. 4(b) is obtained by performing spectrum analysis on an image block of the rotated Lena image (30 degrees), from which the dependencies between two types of peaks can be observed.

Based on the analysis above, we propose to first find the peaks caused by rotation along the four trajectories as (5). However, there may be *false* peaks in these trajectories caused by image content or the interference of two resampling operations. Hence, the found peaks need to be further checked according to the location dependencies describe above. That is, if the peak is indeed introduced by rotation, a corresponding peak introduced by scaling-then-rotation should be found in the line determined by this peak and the corresponding corner. Otherwise, the chance of finding a peak in the line determined by this peak and the corresponding corner is low. Note the peak introduced by scaling-then-rotation should located in a sector from a corner (See the gray area of Fig. 5) according to (6). This prior knowledge in also helpful in eliminating false peaks. The proposed joint estimation method is detailed in Algorithm 1.

IV. Experimental Results

A. Experimental setting

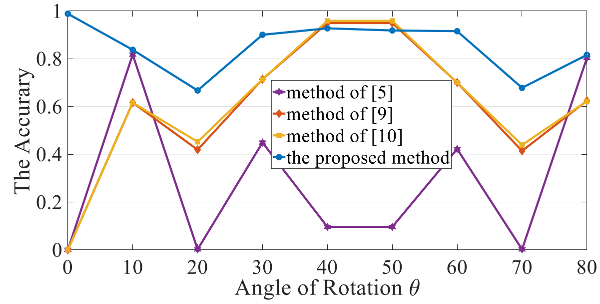

(a)

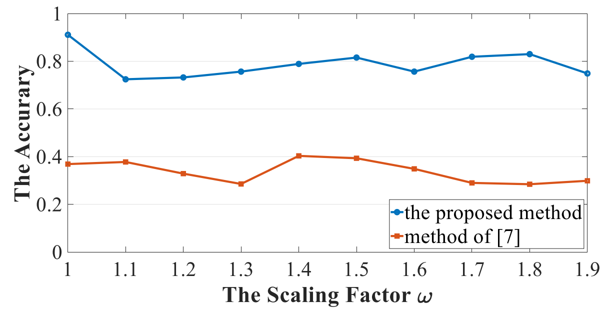

(b)

Fig. 6 The average accuracy of single operation parameter estimation. (a) The propose method is compared with methods [5, 9, 10] on rotation angle estimation. (b) The propose method is compared with method of [7] on scaling factor estimation.

The proposed method is verified on 100 randomly selected images from the BOSSbase dataset [11]. The scaling factor ω varies from 1 to 1.9 with a step of 0.1, and the rotation angle θ varies from $0°$ to $80°$ with a step of $10°$ using the nearest neighbor kernel. In total, $10 \times 9 \times 100 = 9000$ test images are obtained. For the angle estimation, the result is deemed successful when the difference between the estimated angle and the ground truth is smaller than $0.5°$, i.e., $|\hat{\theta} - \theta| < 0.5°$. For the scaling factor estimation, the result is deemed successful when the difference between the estimated factor and the ground truth is smaller than 0.05, i.e., $|\hat{\omega} - \omega| < 0.05$. For the joint estimation, the result is regarded as successful only when it meets the above two criteria simultaneously. For the parameters in the proposed method, we set $N = 40$, $t_1 = 80$, and $t_2 = 50$.[1]

B. Rotation angle estimation and Scaling factor estimation

The proposed method is first compared with state-of-the-art methods [5, 9, 10] in rotation angle estimation. Fig. 6(a) reports the results of the comparative experiment. It can be seen that the proposed method achieves obvious superiority over compared methods, especially in the small angle region. For example, the estimation accuracy of the proposed method is

---

[1] The code is available in https://github.com/yk4023/image_rotation_and_scaling_estimation

98.80% for $\theta=0^{\circ}$, whereas other methods all failed in this case. On average over all angles, the accuracy of our method is 84.96%, and the accuracy of [5], [9], [10] is 29.86%, 59.83%, 60.66% respectively. Such advantage is due to the proposed method can eliminate *false* peaks caused by scaling and rotation interference.

Then the proposed method is compared with the state-of-the-art method [7] in scaling factor estimation. Figure 6(b) reports the results of the comparative experiment, from which obvious advantage of the proposed method can be observed. The average accuracy of our method is 78.88%, and the accuracy of [7] is 33.80%. This is because a large number of peaks are produced by the latter operation (rotation) and the interference of scaling and rotation (See Fig. 4(b)). While the method of [7] only searches the maximum peak, it has a high chance of being misleading. On the contrary, the proposed method fully utilize the dependency between the characteristics of rotation and angle, and thus can eliminate most of the false peaks.

C. *Joint estimation of rotation angle and scaling factor*

The experiments in the last subsection show that the existing single operation parameter estimation methods do not work well for images undergone scaling then rotation. Next, we compare the proposed method with the state of the art of successive operation parameter estimation [12]. We follow [12] to set the threshold τ as 42.3 and the reference table is built with $\omega=1{:}\,0.05{:}\,2$ and $\theta=0{:}\,0.5{:}\,90$ degrees.

Table 1 compares the proposed method and [12] on the joint estimation accuracy under each combination of (ω,θ), and Fig. 7(a) and (b) compare them as a function of ω and θ. At the first glance, the accuracy of the proposed method is slightly inferior to that of [12]. The average accuracies of the proposed method and [12] over all combinations of (ω,θ) are 77.13% and 84.9%, respectively. However, [12] assumes that the ground truth (ω,θ) is included in its reference table, which may not the case in practice. To study this issue, an additional experiment is designed, where the rotation operation parameters keep unchanged, and a small disturbance with maximum value of 0.03 is added to the scaling parameters. For example, the original dataset with $\theta=20^{\circ}$ and $\omega=1.3$ will become $\theta=20^{\circ}$ and $\omega\in[1.27,1.33]$. The results of comparative experiments are shown in Fig.7(b), the solid line is the experimental result of the original dataset, and the dotted line is the experimental result of the disturbed dataset. The joint estimation accuracy of the proposed method and the method of [12] are 70.28% and 57.91%, respectively. It can be seen that the proposed method basically remains stable, while the performance of the method [12] has a significant decline.

It should be note that the joint estimation performance of both methods is poor in some particular cases, e.g., $\omega=1.1$. Through experiments, we find the obtained spectrums are very noisy in these cases, which are likely to mislead the proposed method getting a wrong estimation.

D. *Influence of JPEG Post-Compression*

JPEG compression, which is widely known to have the function of low-pass filtering, can smooth out the forensic

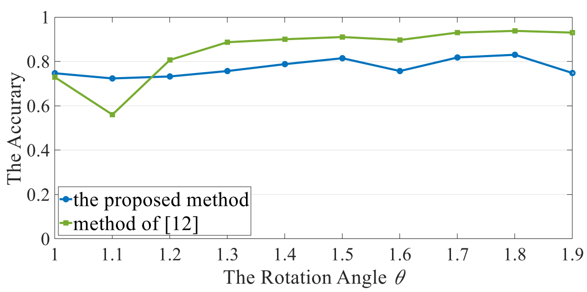

(a)

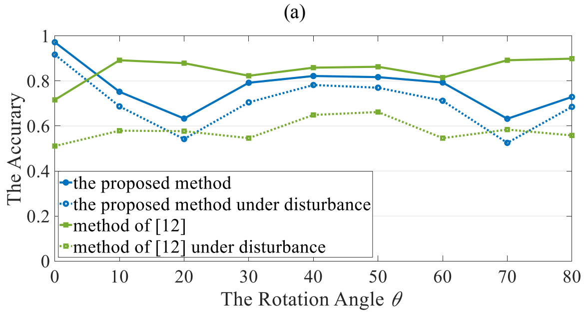

(b)

Fig. 7 The average joint estimation accuracy (a) as a function of the scaling factor $\omega\in[1,\ 1.9]$, (b) as a function of the rotation angle $\theta\in[0°,80°]$. The dotted lines denote the experimental results on the dataset with disturbance added to the scaling factor.

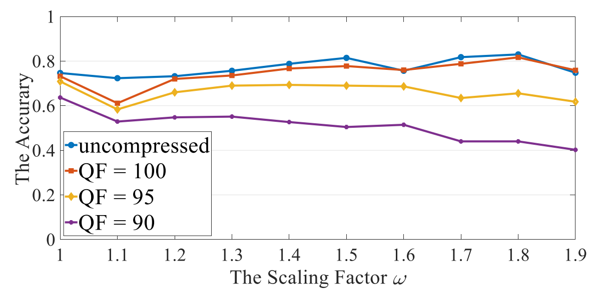

(a)

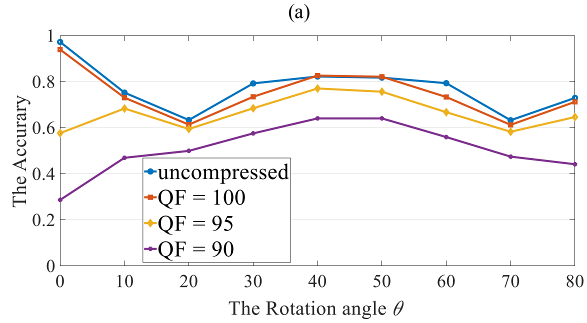

(b)

Fig. 8 The average joint estimation accuracy with the propose method for uncompressed and different JPEG qualities. (a) as a function of the scaling factor $\omega\in[1,\ 1.9]$, (b) as a function of the rotation angle $\theta\in[0°,80°]$.

Table 1 Accuracy (%) comparison (proposed method / [12]) on joint parameter estimation, red color denotes the accuracy lower than or equal 50%

ω/θ	0	10	20	30	40	50	60	70	80
1	80/72	73/83	68/67	69/69	88/67	86/76	71/73	67/78	70/71
1.1	97/58	79/41	71/42	55/57	74/70	74/66	59/47	69/67	73/56
1.2	99/88	76/72	62/62	83/84	65/86	63/85	77/66	64/95	70/88
1.3	98/97	83/86	53/80	74/85	86/93	82/88	78/81	51/99	76/89
1.4	99/100	80/96	69/83	73/84	86/92	86/87	73/82	66/98	77/88
1.5	100/97	76/98	71/83	87/85	82/93	83/90	90/81	67/98	77/94
1.6	100/98	49/92	66/79	92/88	78/92	77/85	92/82	70/97	57/94
1.7	99/97	73/99	74/88	90/87	84/98	85/90	88/83	76/98	67/97
1.8	100/97	84/98	69/90	79/91	91/97	91/90	79/84	71/99	83/98
1.9	100/97	79/97	30/87	90/88	88/97	90/90	86/85	31/99	79/97

traces that our proposed method based on. Moreover, itintroduces new periodicities that will mislead the geometric transform parameter estimation.

Fig. 8 reports the results of the propose method when the geometric transformed images are saved in JPEG format of different quality factors. It is observed that the estimation performance is acceptable when the compression quality is high enough, e.g., the joint estimation accuracies for QF = 100 and 95 are 74.67% and 66.20% respectively, only a few percentage points drop compared with that of uncompressed images. However, the performance may drop significantly if images are more strongly compressed. e.g., the accuracy for QF = 90 is 50.92%, more than 25% blow the uncompressed case. We admit that improving the robustness to JPEG compression is challenging and would like to leave it for future study.

V. Conclusion

Periodic artifacts introduced by scaling and rotation are the most widely used forensics features for geometric transform detection. However, if a probe image has been both scaled and rotated, the forensic features introduced by these two operations will interfere with each other and make the forensic task challenging. In this paper, a joint parameter estimation method is proposed for images undergone scaling-then-rotation. Experimental results show that the proposed method not only has much higher performance than existing methods of estimating the scaling factor and rotation angle separately, but also is less restrictive than the existing joint estimation method. In the future, we plan to extend the joint parameter estimation for images undergone rotation-then-scaling.

Acknowledgment

This work is supported by NSFC (No. 61702429), Doctoral Research Fund of SWUST (No.18zx7163), and China Scholar ship Council (No. 201908515095)

References

[1] A. C. Gallagher, “Detection of linear and cubic interpolation in jpeg compressed images,” in Proc. 2nd Can. Conf. Computer and Robot Vision, 2005, pp. 65–72.

[2] A. C. Popescu and H. Farid, “Exposing digital forgeries by detecting traces of re-sampling,” IEEE Trans. Signal Process., vol. 53, no. 2, pp. 758–767, 2005.

[3] B.Mahdian and S. Saic, “Blind authentication using periodic properties of interpolation,” IEEE Trans. Inf. Forensics Secur., vol. 3, no. 3, pp. 529–538, 2008.

[4] M. Goljan, “Blind detection of image rotation and angle estimation,” in IS&T International Symposium on Electronic Imaging 2018, Media Watermarking, Security, and Forensics. 2018, 158: 1–10.

[5] D. Vázquez-Padín, C.Mosquera, and F. Pérez-González, “Two-dimensional statistical test for the presence of almost cyclostationarity on images,” in Int. Conf. Image Processing, 2010, pp. 1745–1748.

[6] M. Kirchner, “Fast and reliable resampling detection by spectral analysis of fixed linear predictor residue,” ACM Multimedia and Security Workshop, pp. 11–20, 2008.

[7] S. Pfennig and M. Kirchner, “Spectral methods to determine the exact scaling factor of resampled digital images,” in 2012 5th Int. Symp. Communications Control and Signal Processing, 2012, pp. 1–6.

[8] X. Feng, G. Doërr, and I.J. Cox, “An energy-based method for the forensic detection of re-sampled images,” IEEE Int’l Conference on Multimedia and EXPO, 2011.

[9] C. Chen, J. Ni and Z. Shen, “Effective estimation of image rotation angle using spectral method,” in IEEE Signal Processing Letters, 21(7): 890-894, 2014, doi: 10.1109/LSP.2014.2320503.

[10] S. Dai, Y. Zhang, W. Song, et al. “Rotation angle estimation of jpeg compressed image by cyclic spectrum analysis,” Electronics, 2019, 8(12):1431.

[11] P. Bas, T. Filler, T. Pevny, “Break our steganographic system: The ins and outs of organizing BOSS,” in Proc. Int. Conf. on Information Hiding, 2011, pp. 59-70.

[12] C. Chen, J. Ni, Z. Shen and Y. Q. Shi, "Blind Forensics of Successive Geometric Transformations in Digital Images Using Spectral Method: Theory and Applications," in IEEE Transactions on Image Processing, vol. 26, no. 6, pp. 2811-2824, June 2017, doi: 10.1109/TIP.2017.2682963.

[13] W. Wei, S. Wang, X. Zhang and Z. Tang, "Estimation of Image Rotation Angle Using Interpolation-Related Spectral Signatures With Application to Blind Detection of Image Forgery," in IEEE Transactions on Information Forensics and Security, vol. 5, no. 3, pp. 507-517, Sept. 2010, doi: 10.1109/TIFS.2010.2051254.